

## Approximating the average daily surface albedo with respect to soil roughness and latitude

Jerzy Cierniewski<sup>a\*</sup>, Arnon Karnieli<sup>b</sup>, Krzysztof Kuśnierek<sup>a</sup>, Alexander Goldberg<sup>b</sup>,  
and Ittai Herrmann<sup>b</sup>

<sup>a</sup>Department of Soil Science and Remote Sensing of Soils, Institute of Physical Geography and Environmental Planning, Adam Mickiewicz University, 61-680 Poznań, Poland; <sup>b</sup>The Remote Sensing Laboratory, Jacob Blaustein Institutes for Desert Research, Ben-Gurion University of the Negev, Sede-Boker, Israel

(Received 19 November 2010; accepted 1 March 2011)

The present study explores the diurnal variations in blue-sky albedo ( $\alpha$ ) of soils under clear sky conditions with respect to surface roughness. Three roughness levels of ploughed and unploughed soil surfaces, developed from the same loessial material, were examined. The relation between  $\alpha$  of the surfaces and the solar zenith angle, determined during the experiment, enabled us to predict the diurnal  $\alpha$  variation of the surfaces throughout the year at a given latitude, between 75° S and 75° N. The optimal time ( $T_O$ ) for measuring the soil albedo by an instantaneous observation was considered as the best represented time for the daily averaged value within an error lower than  $\pm 2\%$ . It was found that the  $T_O$ , falling at different times depending on the soil surface roughness, limits the possibilities of data achievement by remote-sensing satellites along one of their sun-synchronous orbits.

### 1. Introduction

Surface albedo is the ratio of the amount of solar short-wave radiation reflected from a surface to solar radiation incident upon it. The upwelling and downwelling radiations are integrated over the whole hemisphere (Schaeppman-Strub et al. 2006). Martonchik, Bruegge, and Strahler (2000) recommend using the terms *broadband albedo* or *narrow-band (spectral) albedo* if the albedo characterizes the entire solar short-wave spectrum (0.3–3  $\mu\text{m}$ ) or only a part of it, respectively. The *blue-sky albedo* describes the albedo measured under field conditions, where a surface is illuminated by both direct solar irradiance and diffuse irradiance, scattered by the atmosphere (Baret et al. 2005). This value, characterizing the intrinsic properties of a surface, varies with solar zenith angle, as well as the state of the atmosphere, i.e. clouds and the amount and type of aerosols.

In an early study, Kondratyev (1969) investigated the broadband blue-sky albedo variation of dry rocky and loamy soil surfaces. The albedo of these surfaces decreased from sunrise to midday. When the solar zenith angle decreased from 80° to 60°, their albedo decreased sharply from 22% to 14% and from 34% to 21%, respectively. Furthermore, when the angle decreased to 25°, the albedo dropped smoothly to 11% and 17%, corresponding to the surface type. Mikhaylova and Orlov (1986) found that soil surface

---

\*Corresponding author. Email: ciernje@amu.edu.pl

reflectance increases with decreasing soil particle size, because large aggregates have an irregular shape with a higher number of inter-aggregate spaces and cracks, where the incident radiation is trapped. The higher the roughness of the soil surfaces, the lower their albedo. A similar relation between the narrowband albedo of soil surfaces and solar zenith angle and soil surface roughness was confirmed by Pinty, Verstraette, and Dickinson (1989), Lewis and Barnsley (1994), and Wang, Barlage, and Zeng (2005).

Year-round variations of soil albedo values, generated by a hemispherical-directional reflectance model (Cierniewski, Gdala, and Karnieli 2004), from midday to sunset under clear sky conditions in different latitudes, are presented in Cierniewski and Gdala (2010). These data are predicted for virtual surfaces representing smooth, moderately rough, and very rough soils, located between  $75^{\circ}$  S and  $75^{\circ}$  N. Irregularities of the surfaces were simulated by three parameters describing their height variation by the amplitude of the sinus function along the  $x$ - and  $y$ -axes, as well as the disturbance in their height variation. The model of Cierniewski, Gdala, and Karnieli (2004) assumes that a virtual surface is illuminated by the hemispherical radiation created by a number of point radiation sources of given radiation equally spread around the hemisphere. The amount of energy reflected only once from an elementary fragment of the surface depends on the angle between the direction of the incoming irradiation and the normal at any given point of the fragment. The radiation leaving each fragment of the surface is scattered in accordance with the quasi-Lambertian function. The entire radiation reflected from the whole surface and viewed by a sensor along a direction is the sum of all vectors of the radiation reflected along this direction from each elementary fragment of the surface due to its illumination by each unblocked point radiation source. The results of the modelling under the simplifying assumption that the electromagnetic irradiation is only once reflected from rough soil surfaces require verification in natural conditions.

As a further continuation of the study of Cierniewski and Gdala (2010), this article explores the relation between the broadband blue-sky soil albedo and the solar zenith angle, based on field measurements under clear sky conditions.

## 2. Methods

Measurements were conducted on soil surfaces in the Israeli Negev desert, near Sede Boker in Israel ( $30^{\circ} 51' 26''$  N,  $34^{\circ} 47' 09''$  E). The area is characterized by loessial substrate (Issar et al. 1984). Specifically, the study was carried out over unploughed and ploughed soil surfaces with three levels of surface roughness: smooth, moderately rough (after shallow ploughing), and very rough (after deep ploughing) soils (Figure 1).

The blue-sky albedo of the soil surfaces was measured by an albedometer LP PYRA 06 (Delta Ohm, Padua, Italy) in the spectral range of  $0.335\text{--}2200\ \mu\text{m}$ . The instrument, consisting of one down-facing and one up-facing LP PYRA 03 pyranometer, was installed 2 m above the ground. Data were recorded by a Campbell Scientific 21x data logger.

Surface roughness of the three surfaces was measured using a VIVID-910 laser scanner (Konica-Minolta, Tokyo, Japan). The scanner was placed on a tripod that was moved around to read a  $1\ \text{m}^2$  plot from four different directions. Owing to technical constraints related to the scanner's working conditions, the 3D measurements were conducted in the dark, after sunset, using a fluorescent lamp (Figure 2).

The textural composition of the soil surface material was analysed in the laboratory using a hydrometer, the organic carbon content by Walkley Black's method, calcium carbonate equivalent by Piper's method, and the total 'free' iron oxide by the citrate-dithionite-bicarbonate (CDB) method of Mehra and Jackson, as described by Sparks et al. (1996).

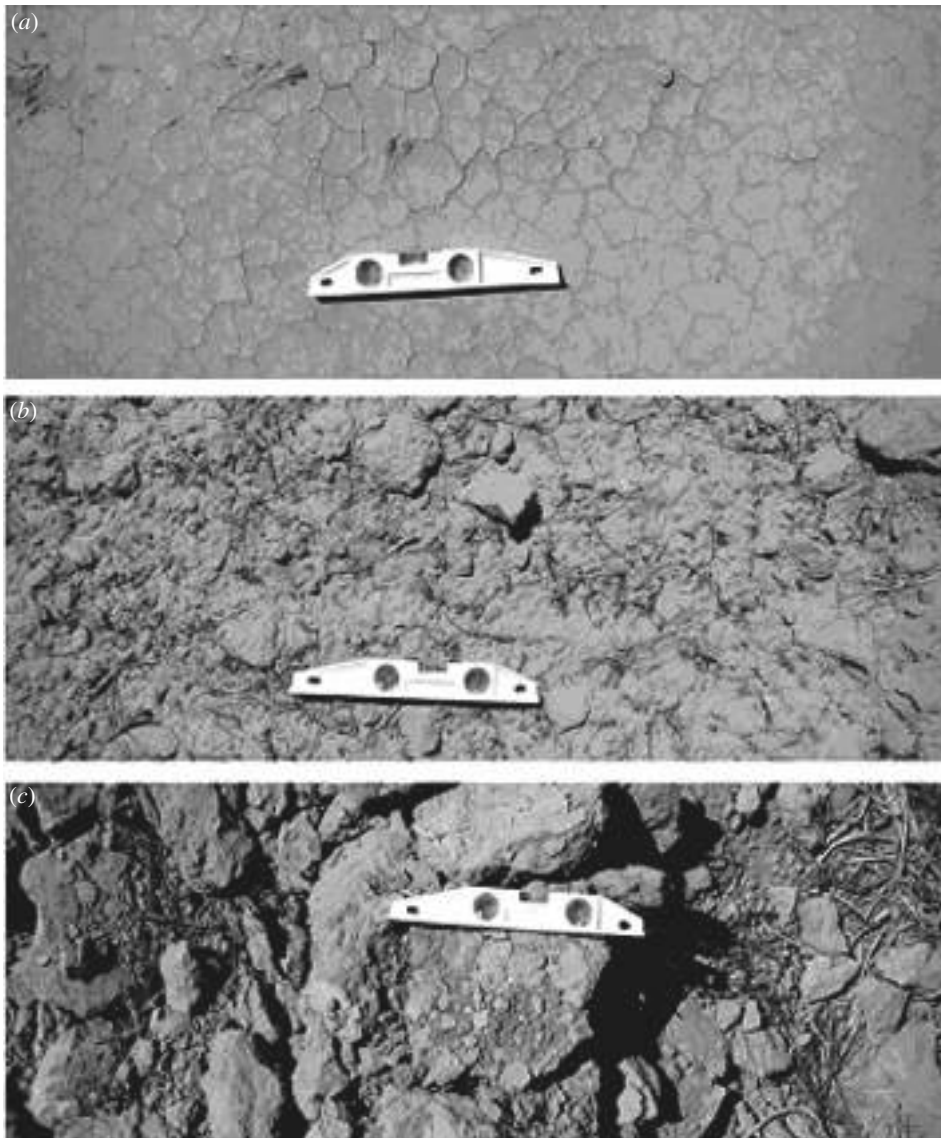


Figure 1. Tested soil surfaces: (a) smooth; (b) moderately rough; and (c) rough. A level 30 cm long is shown as a reference.

### 3. Results and discussion

Physical and chemical properties of the soil, which have a significant influence on the reflectance features, were very similar for all the tested surfaces (Table 1).

The 3D scanner source data of the surfaces were transformed to a set of points with  $x$ ,  $y$ , and  $z$  coordinates. Based on the point data, a digital elevation model (DEM) of the surfaces was computed with 1 mm horizontal and vertical spatial resolution. The DEM was used to characterize the shape of the studied surfaces quantitatively using the following indices: height standard deviation (HSD), ratio of the total surface area to the total projected area (RTS), height variogram range (RHV), and sill parameters (SHV). The computed index values are presented in Table 2.



Figure 2. (a) 3D measurement set-up of Konica-Minolta VIVID-910 laser scanner and (b) scanner head.

Table 1. Properties of the tested soils with smooth (S), moderately rough (M), and very rough (R) surfaces.

Soil property	S	M	R
Sand (2–0.05 mm) (%)	45	46	48
Silt (0.05–0.002 mm) (%)	45	42	40
Clay (<0.002 mm) (%)	10	12	12
Organic carbon (%)	0.5	0.87	0.92
CaCO <sub>3</sub> (%)	30.7	30.1	28.1
Fe <sub>2</sub> O <sub>3</sub> (%)	1.48	1.51	1.52
Soil Munsell dry colour	10YR7/4	10YR7/4	10YR7/4

Table 2. Values of shape indices for the studied surfaces: smooth (S); moderately rough (M); and very rough (R).

Shape indices	S	M	R
HSD (mm)	0.54	10.43	46.73
RTS	1.01	1.2	1.72
RHV (mm)	101.69	572.57	1017.35
SHV (mm <sup>2</sup> )	0.3	101.34	192.30

The measurements of the blue-sky albedo,  $\alpha$ , of the surfaces were carried out on 8–12 August 2008 under clear sky conditions from local noon to sunset at 1 min intervals. Variation of the measured  $\alpha$  as a function of the solar zenith angle,  $\theta_s$ , is presented in

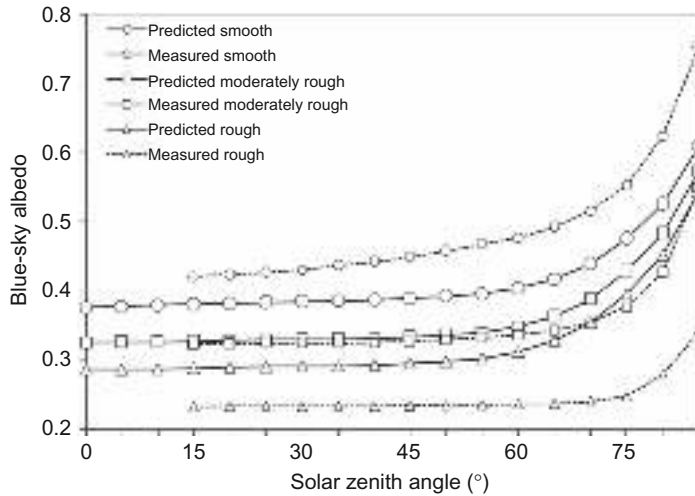


Figure 3. Variation of the blue-sky albedo as a function of the solar zenith angle measured and predicted by the hemispherical-directional reflectance model.

Figure 3. The measured  $\alpha$  data are demonstrated on the background of a similar relation, but predicted by the hemispherical-directional reflectance model using the virtual surfaces discussed in Cierniewski and Gdala (2010). The modelling curves are parallel to each other, although they have different levels (Figure 3). The highest level depicts the curve of the smooth surface, and the lowest one the curve of the very rough surface. The measured curves have a similar shape, but they are not as parallel as the modelling curves. The measured curve related to the extremely rough surface (characterized by the highest values of the shape indices) does not rise at  $\theta_s$  angles lower than  $75^\circ$ , while for the extremely smooth surface (of the lowest values of the indices) the curve increases throughout the analysed  $\theta_s$  range. The measured smooth curve increases markedly at  $\theta_s$  angles higher than  $65^\circ$ . The measured  $\alpha$  variation for the moderately rough surface is similar to the variation predicted by the model using the virtual surface; however, the increase is noticed at  $\theta_s$  higher than  $75^\circ$ . The disagreement in the  $\alpha$ - $\theta_s$  dependence obtained by the modelling and the measured data justifies the continuation of the study of Cierniewski and Gdala (2010). The soil  $\alpha$  variation measured for the moderately rough surfaces is treated in the further analysis as the base pattern to assess modelling and measured effects of soil surface roughness on the optimal time  $T_O$  for the average daily soil albedo  $\bar{\alpha}$  approximation. The  $T_O$  is defined as the time when the  $\alpha$  acquired by an instantaneous observation best represents the  $\bar{\alpha}$  value calculated during the day from sunrise to sunset.

Cierniewski and Gdala (2010) showed that the roughness of the virtual surfaces does not influence the optimal time  $T_O$  required for the  $\alpha$  approximation. The measured soil albedo distributions in the  $\theta_s$  function change the previous findings concerning the  $T_O$  of soil surfaces in the context of their roughness. In this paper, we used the same procedure of the  $T_O$  prediction as in the previous paper. The optimal time  $T_O$  was re-calculated in 5 min intervals and  $5^\circ$  latitude increments in the northern (NH) and southern hemispheres (SH) between the latitude,  $L$ , angles of  $75^\circ$  for the same four dates of the year 2000, 21 March, 16 April, 7 May, and 22 June, as in the previous study (Cierniewski and Gdala 2010). The dates 21 March and 22 June relate in the NH to the astronomical spring equinox and the beginning of the astronomical summer, respectively. The day of 16 April characterizes a

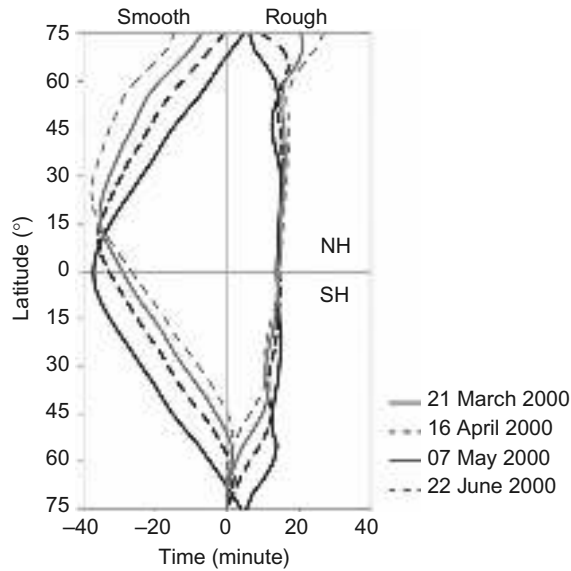


Figure 4. Time intervals in minutes determined with respect to the optimal time  $T_O$  in the afternoon for real smooth and rough soil surfaces with respect to the moderately rough surface, as a function of latitude in the northern (NH) and southern (SH) hemispheres for selected days in the year 2000.

clearly different pattern of the albedo distribution in comparison to the dates mentioned above. Additionally, the day of 7 May is a date halfway between the astronomical spring equinox and the beginning of the astronomical summer in the NH.

Figure 4 shows that the optimal time calculated for the real surfaces depends on their roughness. The differences between  $T_O$  for the extremely rough ( $T_{OR}$ ) and smooth ( $T_{OS}$ ) surfaces are expressed as relative to the optimal time for the moderately rough surface ( $T_{OM}$ ). In the afternoon, the relative  $T_O$  for the smooth soil surface  $T_{OS}-T_{OM}$  falls earliest (reaching its negative values), whereas for the rough surface  $T_{OR}-T_{OM}$  it falls latest (reaching its positive values). In the morning this trend is reversed. The  $T_{OS}-T_{OM}$  is clearly higher than  $T_{OR}-T_{OM}$ . The  $T_{OS}-T_{OM}$  shows a great variation in the  $L$  function and its difference for the tested dates. It reaches its maximum nearly 40 min from the  $L$  of about  $10^\circ$  (SH) to  $20^\circ$  (NH). The  $T_{OS}-T_{OM}$  reaches lower values towards higher  $L$  in the NH and the SH. The  $T_{OR}-T_{OM}$  reaches only about 15 min within the  $L$  range between  $45^\circ$  (SH) and  $60^\circ$  (NH) and is almost constant in this range for all the tested dates.

In Cierniewski and Gdala (2010), the optimal time approximation for achieving the average daily soil albedo for surfaces varying with the latitude was considered with its accuracy error,  $\varepsilon$ , lower than  $\pm 2\%$ . This error level was determined by Sellers et al. (1995) as the required accuracy for global climate modelling. The present study explores whether the achievement of the average daily albedo for the rough and smooth surfaces may be assessed with an  $\varepsilon$  lower than  $\pm 2\%$  using the optimal time adequate for the moderately rough surface. The graphs in Figure 5 present  $T_O$  distribution calculated for the moderately rough surfaces in the  $L$  function with its  $\pm 2\%$  error lines. The distributions for the smooth surface,  $T_{OS}$ , and the very rough surface,  $T_{OR}$ , complete the graphs to check in which  $L$  range they exceed the acceptable lines of  $\pm 2\%$  error specified for the moderately rough surface. The optimal time for  $T_{OR}$  does not exceed these  $\pm 2\%$  error limits for all the tested dates. The  $T_{OR}$  presents a similar distribution to the moderately rough surface with

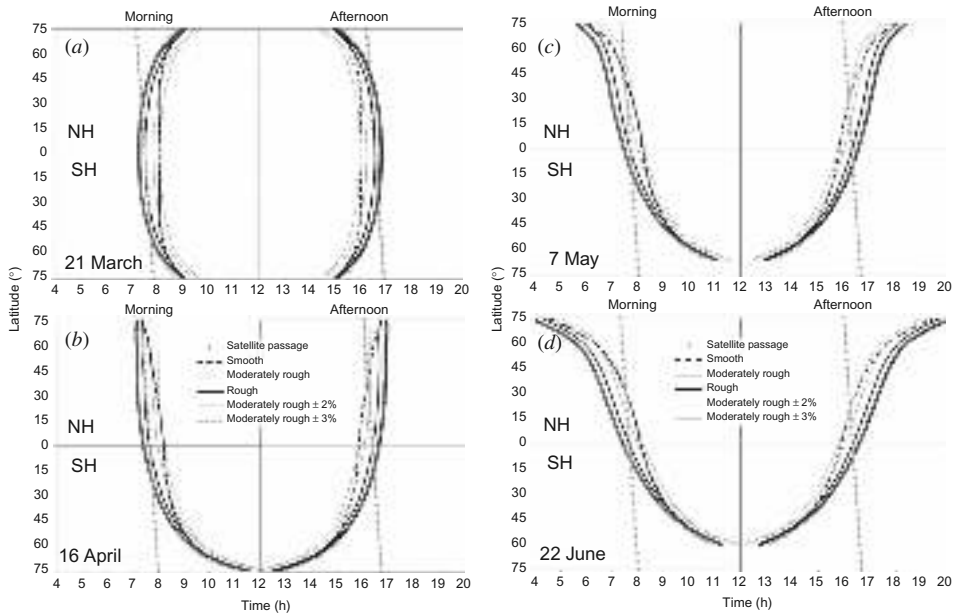


Figure 5. Time in the hour scale of GMT when, for the chosen days (a) 21 March, (b) 16 April, (c) 7 May, and (d) 22 June, the average daily soil surface albedo  $\bar{\alpha}$ , varying with the latitude, is available to be assessed with the error lower than  $\pm 2\%$  and  $\pm 3\%$  (dashed lines). The dotted lines depict the time of the remote-sensing satellite passage crossing the equator exactly at the optimal time for the latitude  $0^\circ$ . NH and SH describe the northern and southern hemispheres, respectively.

its  $-2\%$  error in the morning and  $+2\%$  error in the afternoon. It can be interpreted that the optimal time predicted for the moderately rough surface is also useful to achieve the average daily albedo with its acceptable error for very rough surfaces, even for those extremely rough surfaces that were measured during the discussed experiment. The  $T_{OS}$  distribution predicted for the smooth surface exceeds  $\pm 2\%$  error limits in the following latitude ranges:  $35^\circ$  S– $35^\circ$  N,  $30^\circ$  S– $45^\circ$  N,  $20^\circ$  S– $50^\circ$  N, and  $15^\circ$  S– $60^\circ$  N for 21 March, 16 April, 7 May, and 22 June 2000, respectively. Furthermore, in the ranges where the  $\varepsilon$  was higher than  $\pm 2\%$ , we tried to express the maximum  $\varepsilon$  value quantitatively. Therefore, additional error levels in steps of  $0.2\%$  were iteratively added to the distributions. It was found that the maximum  $\varepsilon$  associated with the  $T_{OS}$  distribution does not exceed  $3\%$ . These  $\pm 3\%$  error lines are drawn in Figure 5.

As in Cierniewski and Gdala (2010), we also considered the practical implications following the acceptable time intervals for evaluation of the average daily albedo,  $\bar{\alpha}$ , of soil surfaces with various roughnesses by satellite technology, over a wide latitude range. A remote-sensing satellite on a typical sun-synchronous orbit with its 98 min period (e.g. Landsat TM/ETM+) was analysed, assuming for example that the satellite crosses the equator exactly at the optimal time for the four chosen dates for the moderately rough surface. This surface was judged as representative of many soil surfaces with a wide roughness range, with the exception of only extremely smooth surfaces similar to that tested in the studies and discussed above. It was determined from which part of that orbit, expressed by the length of the latitude range, the remote-sensing satellite can collect the  $\bar{\alpha}$  with its acceptable  $\pm 2\%$  error. The results of the assessment are presented in Figure 5. This length of the orbit part is described between intersection points of two kinds of lines: the dotted

Table 3. The length of a remote-sensing satellite orbit at which it can collect the average daily albedo,  $\bar{\alpha}$ , of soil surfaces with its acceptable  $\pm 2\%$  error.

Date	Morning		Afternoon	
	Measured ( $^{\circ}$ )	Predicted ( $^{\circ}$ )	Measured ( $^{\circ}$ )	Predicted ( $^{\circ}$ )
21 March	70	60	70	60
16 April	95	>90	40	20
7 May	45	25	25	15
22 June	25	20	15	10

line, defining the time of the satellite passage at various  $L$ , and the dashed lines, describing the limits of the acceptable  $\pm 2\%$  error. The higher the convergence of the two kinds of lines, the higher the orbit part length sought for the analysed dates. The results obtained in this article are not significantly different in comparison to Cierniewski and Gdala (2010) (Table 3).

Overall, the measured albedo data in comparison to the modelling data provide a slight increase of the length of a remote-sensing satellite orbit at which the  $\bar{\alpha}$  of soil surfaces can be assessed with an acceptable  $\pm 2\%$  error for all chosen dates. The longest,  $95^{\circ}$ , part of the orbit is predicted for the morning of 16 April, while the shortest,  $15^{\circ}$ , part of the orbit is expected for the afternoon of 22 June. For both dates, the orbit lengths verified by the measured data are only  $5^{\circ}$  longer than the length determined by the model. For other tested dates, the orbit length increases by  $5\text{--}20^{\circ}$ .

#### 4. Concluding remarks

The soil albedo  $\alpha$  variation as a function of the solar zenith angle  $\theta_s$  obtained directly by field measurements is different from the variation predicted by the hemispherical-directional reflectance model using virtual soil surfaces. The measured curve of the extremely rough surface almost does not rise at the  $\theta_s$  angles lower than  $75^{\circ}$ , while the curve of the extremely smooth surface increases throughout the analysed  $\theta_s$  range, rising strongly at the  $\theta_s$  angles higher than  $65^{\circ}$ . The measured  $\alpha\text{--}\theta_s$  dependence for the moderately rough surface is similar to the dependence predicted by the model using the virtual surface; however, its increase is noticed at  $\theta_s$  higher than  $75^{\circ}$ .

The measured data, contrary to the modelling data, show that the optimal time  $T_O$  for evaluation of the average daily soil albedo  $\bar{\alpha}$  differs in dependence on the roughness of the studied soil surfaces. In the afternoon,  $T_{OS}$  for the smooth soil surface declines earlier each day than for the moderately rough  $T_{OM}$ , whereas for the very rough one,  $T_{OR}$ , it declines later than for  $T_{OM}$ . In the morning this trend is reversed. In certain latitude ranges, the difference between  $T_{OS}$  and  $T_{OM}$  does not exceed 40 min, while that between  $T_{OR}$  and  $T_{OM}$  is 15 min. It was found that using the optimal time predicted for the moderately rough surface,  $T_{OM}$ , taking into consideration its  $\pm 2\%$  error, it is also possible to achieve the  $\bar{\alpha}$  for very rough surfaces, even for the extremely rough surface that was measured during the discussed experiment. It was found that the use of the  $T_{OM}$  for the achievement of the smooth surface  $\bar{\alpha}$  is possible in the whole latitude range analysed with a higher error, reaching  $\pm 3\%$ .

The optimal time for evaluating the  $\bar{\alpha}$ , determined here depending on the roughness of a surface and its latitudinal position, opens up the possibilities of using remote-sensing satellites along one of their sun-synchronous orbits for data acquisition. Overall, the measured

albedo distribution in relation to the modelling distribution gives a slight increase of the length of a remote-sensing satellite orbit at which the average daily albedo of soil surfaces can be collected with the acceptable  $\pm 2\%$  error. The longest part of the orbit, calculated by the measured data, was estimated as about  $95^\circ$ . It was predicted for the morning of 16 April, while the shortest length, reaching only about  $15^\circ$ , was expected for the afternoon of 22 June, i.e.  $5^\circ$  longer in relation to the prediction using modelling data.

### Acknowledgements

This work was carried out within the framework of the projects 2 P04E 030 29 and NN 306013637, supported by the Polish Ministry of Science and Higher Education and by the 'Sixth EU Framework Programme – Transnational Access implemented as Specific Support Action – Dryland Research' (EC contract number 026064).

### References

- Baret, F., C. Schaaf, J. Morisette, and J. Privette. 2005. "Report on the Second International Workshop on Albedo Product Validation." *The Earth Observer* 17: 13–17.
- Cierniewski, J., and T. Gdala. 2010. "Calculating the Optimal Time When Albedo Approximates Its Daily Average: An Example Using Soil Surfaces with Various Roughnesses at Different Latitudes." *International Journal of Remote Sensing* 31: 2697–708.
- Cierniewski, J., T. Gdala, and A. Karnieli. 2004. "A Hemispherical-Directional Reflectance Model as a Tool for Understanding Image Distinctions between Cultivated and Uncultivated Bare Surfaces." *Remote Sensing of Environment* 90: 505–23.
- Issar, A., A. Karnieli, H. J. Bruins, and I. Gilead. 1984. "The Quaternary Geology of Sede-Zin, Negev, Israel." *Israel Journal of Earth Science* 33: 34–42.
- Kondratyev, K. Y. 1969. "Albedo zemnoy poverkhnosti i oblokov." In *Radiacjonnyje Charakteristiki Atmosfery i Zemnoy Poverkhnosti*, edited by Z. F. Miranova, 176–224. Leningrad: Gidrometeorologicheskoye Izdatelstwo.
- Lewis, P., and M. J. Barnsley. 1994. "Influence of the Sky Radiance Distribution on Various Formulations of the Earth Surface Albedo." In *Proceedings of the 6th International Symposium on Physical Measurements and Signatures in Remote Sensing*, edited by G. Guyot, January 17–21, Val d'Isere, France, 707–15. Paris: CNES.
- Martonchik, J. V., C. J. Bruegge, and A. Strahler. 2000. "A Review of Reflectance Nomenclature Used in Remote Sensing." *Remote Sensing of Environment* 19, 9–20.
- Mikhaylova, N. A., and D. S. Orlov. 1986. *Opticheskie Svoystva Pochv i Pochvennykh Komponentov*. Moskva: Nauka.
- Pinty, B., M. M. Verstraete, and R. E. Dickinson. 1989. "A Physical Model for Predicting Bidirectional Reflectance over Bare Soil." *Remote Sensing of Environment* 27: 273–88.
- Schaepman-Strub, G., M. E. Schaepman, T. H. Painter, S. Dangel, and J. V. Martonchik. 2006. "Reflectance Quantities in Optical Remote Sensing – Definitions and Case Studies." *Remote Sensing of Environment* 103: 27–42.
- Sellers, P. J., B. W. Meeson, F. G. Hall, G. Asrar, R. E. Murphy, R. A. Schiffer, F. P. Bretherton, R. E. Dickinson, R. G. Ellingson, C. B. Field, K. F. Huemmrich, C. O. Justice, J. M. Melack, N. T. Roulet, D. S. Schimel, and P. D. Try. 1995. "Remote Sensing of the Land-Surface for Studies of Global Change: Models-Algorithms-Experiments." *Remote Sensing of Environment* 51: 3–26.
- Sparks, D. L., Page, A. L., Helmke, P. A., Loeppert, R. H., Soltanpour, P. N., Tabatabai, M. A., Johnston, C. T., and Summer, M. E., eds. 1996. *Methods of Soil Analysis. Part 3. Chemical Methods*. Madison, WI: Soil Science Society of America and American Society of Agronomy.
- Wang, Z., M. Barlage, and X. Zeng. 2005. "The Solar Zenith Angle Dependence of Desert Albedo." *Geophysical Research Letters* 32: L05403.